# An ionic concentration and size dependent dielectric permittivity Poisson-Boltzmann model for biomolecular solvation studies

**ARTICLE** *in* THE JOURNAL OF CHEMICAL PHYSICS · JULY 2014

Impact Factor: 2.95 · DOI: 10.1063/1.4887342 · Source: PubMed



**2 AUTHORS:**

Hanlin Li
Chinese Academy of Sciences
**2** PUBLICATIONS **5** CITATIONS

SEE PROFILE

Benzhuo Lu
Chinese Academy of Sciences
**52** PUBLICATIONS **997** CITATIONS

SEE PROFILE

# An ionic concentration and size dependent dielectric permittivity Poisson-Boltzmann model for biomolecular solvation studies

Hanlin Li and Benzhuo Lu[a)]

*State Key Laboratory of Scientific and Engineering Computing, Institute of Computational Mathematics and Scientific/Engineering Computing, National Center for Mathematics and Interdisciplinary Sciences, Academy of Mathematics and Systems Science, Chinese Academy of Sciences, Beijing 100190, China*

(Received 7 April 2014; accepted 25 June 2014; published online 14 July 2014)

By considering the influence of volume exclusion on the solvent dielectric, a variable dielectric Poisson-Boltzmann (VDPB) model is explored for molecular solvation studies by using a dielectric as an explicit function of ionic sizes and concentrations. A finite element method is adopted and an iterative strategy is introduced to numerically solve the VDPB equation. According to our computations, the current dielectric model can result in considerable differences compared with the traditional Poisson-Boltzmann (PB) solutions, especially for those systems with highly charged biomolecule and/or under high salt concentration condition. The model to certain extent captures the fact of dielectric decrement of electrolyte solutions, which is especially remarkable in the vicinity of molecules. Counter-ion concentration very near the molecular surface in VDPB calculation is found higher than that in PB. The new dielectric model may also influence the charge compensation behavior near biomolecular surface. For a spherical cavity solvated in a concentrated ionic solution, charge inversion is observed in VDPB, which does not occur with the traditional PB model. Besides, the solvation energy predicted by VDPB will always be greater than that by PB. Moreover, differing from PB, the VDPB also allows non-monotonous dependencies of solvation energy on ionic strength.
 [http://dx.doi.org/10.1063/1.4887342]

## I. INTRODUCTION

Numerous processes involving the bending, folding, melting, and binding of highly charged polyelectrolyte, are of great importance for biological functions. These processes are strongly influenced by changes in the ionic solvent environment. Nonspecific salt-mediated electrostatic interactions play a critical role in these biomolecular processes, and such interactions largely govern the complex salt-dependent behavior of the above-mentioned processes. Therefore, physically realistic models of these electrostatic interactions are essential to predict the physiochemical behavior of charged biomacromolecule in ionic solutions.

The Poisson-Boltzmann (PB) equation has been extensively used to model the ionic solvent environment of biomolecule due to its simplicity and ability to accurately predict many thermodynamic properties.[1–8] However, it is still an approximation model and does not take into account finite ion size and ion-ion correlation effects, which prohibit its application to systems where these effects become pronounced such as ionic layering, overcharging, or charge inversion, like-charge attraction, and ion selectivity inversion.[9–15] In particular, the assumption that the continuum dielectric medium is homogeneous does not take into account the strong dielectric response of water molecules around charged particles. The discrete moments of water molecules will orient themselves close to charged particles and surfaces giving rise to hydration shells, which can be measured at short distances. These hydration phenomena are very important in many biological processes such as protein folding, protein crystallization, and interactions between charged biopolymers inside the cell.[16] Theoretical and experimental evidences also show that in a considerably wide region of the solution away from protein/membrane/DNA molecules the dielectric coefficient can be much lower than pure water.[17–20]

In the past few decades, some works are devoted to modify the PB equation in a relatively simple way to consider the strong dielectric response of aqueous salt solution. The effect of variable dielectric coefficient and finite ion size on PB calculations is studied in 1993.[21] In the work, the dielectric coefficient is not a continuous function but takes piecewise constants. In a recent work, a Gaussian-based approach was implemented to deliver a smooth dielectric coefficient distribution across the interface between protein and surrounding water phase by utilizing the 3D structure of the corresponding macromolecule.[22] Besides, an alternative way of dealing with the limits of PB is to consider ions explicitly in the PB calculations. Their position can be predicted and to be considered as part of protein structure.[23]

So far there have been extensive studies of physical properties of aqueous electrolyte solutions. The first systematic experimental study of the dielectric properties of salt-water solutions was conducted in 1948 by Hasted *et al.*[24] In the work, the static dielectric constant of a solution was observed to decrease with the salt concentration, a phenomena called dielectric decrement. Intuitively, the dielectric decrement stems from the fact that the local electric field generated by each

a)Author to whom correspondence should be addressed. Electronic mail: bzlu@lsec.cc.ac.cn

 

ion dominates the external applied field. The polar water molecules tend to align with the local ionic field, creating a hydration shell around the ion. The ions provide specific interactions to the surrounding water molecules and thus restricting their motion and ability to respond to external electrostatic field, hence lowering the dielectric permittivity. In dilute solutions, the dielectric decrement is found linear,

$$\epsilon_V = \epsilon_w - \alpha c, \tag{1}$$

where $\epsilon_w$ is the relative permittivity of pure water, $c$ is the salt concentration, and $\alpha$ is a phenomenological ion-specific parameter, known as the total excess polarization of the ionic species. At higher salt concentrations, significant deviations from linearity are observed and the dielectric decrement is observed to saturate. The model was then refined by considering the variation of the local dielectric constant near the ions[25] and finite-size effects.[26] Besides, Levesque *et al.*[27] developed a model for electrolyte solutions in which the dielectric permittivity was determined from a part of the dipole fluctuation of a solution by considering the contribution of the water molecules only, which took the form

$$\epsilon_E(c) = \frac{\epsilon_w}{1 + \alpha \cdot c}, \tag{2}$$

where $\epsilon_w$ is the relative permittivity of pure water, $c$ is the salt concentration, and $\alpha$ is a fitted parameter. It turns out that the physical effects of electrolyte solutions can be captured well by $\epsilon_E(c)$.[28] Considering the fact that at higher salt concentrations significant deviations from linearity are observed and the dielectric decrement is observed to saturate,[24] $\epsilon_E$ is a more accurate dielectric permittivity model than the linear $\epsilon_V$. However, both models reflect the observed phenomenon of dielectric decrement. And for dilute electrolyte solutions the difference between $\epsilon_E$ and $\epsilon_V$ is negligibly small.

The above two dielectric models for electrolyte solution have not been explored for biomolecular solution system, especially in PB solvation calculations. In this work, an effort was made to find a continuum function of dielectric permittivity with a more natural and physical basis that can capture well the dielectric response of aqueous salt solution so that such a variable dielectric permittivity can be applied to PB calculations. By considering the ionic solution as a mixture of high dielectric material (water dipoles) and low dielectric material (ions and hydration shells), we obtain a variable dielectric PB ($\text{VDPB}_V$) equation in which $\epsilon$ is an explicit function of ionic concentrations and ionic effective sizes that incorporates the hydration shell effects. Similarly, by simply adopting the concentration dependent dielectric permittivity of Levesque *et al.*,[27] we obtain another variable dielectric PB ($\text{VDPB}_E$) equation (see Sec. II for details). Here, "simply adopting" means that the type of dielectric permittivity form as by Levesque *et al.*[27] or many others are derived for pure electrolyte system, where there is no biomolecule existed and no external electric field considered, and the system is locally neutral in charge everywhere. But in $\text{VDPB}_E$ for biomolecular system, we still use the dielectric permittivity form despite the brokenness of local neutrality (no balance in composition of positive charges and negative charges). Whereas in $\text{VDPB}_V$, it is relatively simple and there is no such neutrality considerations in principle. Comparisons are made between these two variable dielectric permittivity PB models and the traditional piecewise constant dielectric PB models. A finite element method is adopted to numerically solve the equation. It is worth noting that in the VDPB equation the dielectric coefficient depends exponentially on the electric potential, i.e., the solution of the equation. As a result, the VDPB equation is of strong nonlinearity. Using Newton method to directly solve the equation will encounter convergence difficulty, an iterative strategy is introduced instead. We aim to apply the VDPB equation to study the solvation of irregular shaped biomolecules in ionic solution with possible multiple ion species. Numerical experiments are carried out for a spherical cavity and a DNA duplex. According to our computations, the current variable dielectric models can result in considerable differences compared with the traditional PB solutions, e.g., charge inversion and non-monotonous dependencies of solvation energy on ionic strength can be observed in VDPB results, which cannot occur in the traditional PB model. The differences are especially significant for those systems with highly charged biomolecule and/or under high salt concentration conditions.

The rest of this paper is organized as follows. In Sec. II, two VDPB models are introduced and discussed. In Sec. III, comparisons are made between the predictions of the two VDPB models and the traditional PB. Finally, conclusions are drawn in Sec. IV.

## II. METHODS

The nonlinear Poisson-Boltzmann equation takes the form

$$-\nabla \cdot (\epsilon(r)\nabla\phi(r)) = \rho^f(r) + \lambda \sum_{i=1}^{K} q_i c_i^{\infty} e^{-q_i \beta \phi(r)}, \text{ in } \Omega. \tag{3}$$

Fig. 1 illustrates a biomolecular solution system occupying domain $\Omega$ with a smooth boundary $\partial\Omega$. Domain $\Omega_s$ denotes the solvent region that contains several diffusing species

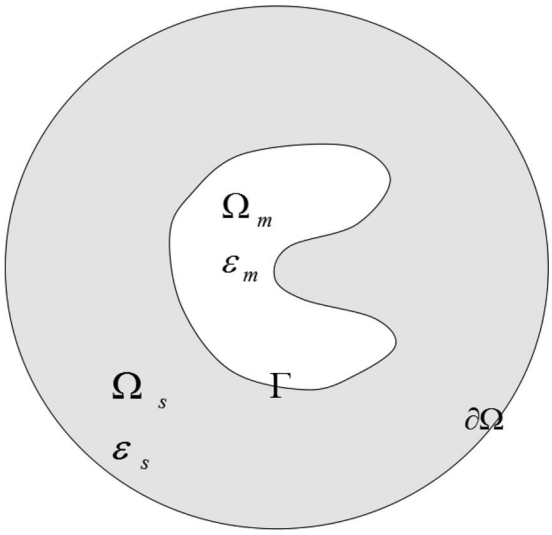


FIG. 1. Schematic illustration of the computational domain.

and domain $\Omega_m$ denotes the biomolecular region. Here, $\Omega = \Omega_s \cup \Omega_m$ and $\Gamma$ denotes the boundary of $\Omega_m$. Besides, $c_i^\infty$ is the bulk ionic concentration of the $i$th ionic species, $\lambda = 0$ in the biomolecular region $\Omega_m$ and $\lambda = 1$ in the solvent region $\Omega_s$, $K$ is the number of ionic species considered, $\beta = 1/k_BT$ is the inverse Boltzmann energy, $k_B$ is the Boltzmann constant, $T$ is temperature, $\phi(r)$ is the electrostatic potential, $q_i = z_i e_c$ is the charge of each particle of the $i$th ionic species, $e_c$ is the elementary charge, $z_i$ is the valence of the $i$th ionic species, $\rho^f(r) = \sum_{j=1}^{S} Q_j \delta(r - r_j)$ is an ensemble of point charges $Q_j$ located at $r_j$ inside $\Omega_m$ ($j = 1, 2, \ldots, S$), $S$ is the number of point charges, $\delta(\ \cdot\ )$ is the Dirac Delta function, and $\epsilon(r)$ is the dielectric coefficient distribution function.

In most practically used PB models in computational chemistry and biophysical communities, the dielectric coefficient is usually taken as piecewise constants dependent on regions

$$\epsilon = \begin{cases} \epsilon_m, & \text{in } \Omega_m, \\ \epsilon_s, & \text{in } \Omega_s. \end{cases}$$

However, due to insertion of finite sized ions and the strong dielectric response of water molecules around charges and other effects, the static dielectric constant of a solution will decrease with the salt concentration, a phenomena called dielectric decrement.

Recall the linear dielectric permittivity, $\epsilon(c) = \epsilon_w - \alpha c$, $\alpha$ is a phenomenological ion-specific parameter which determines how fast the dielectric permittivity decreases with concentration. Note that the unit of $\alpha$ is Å$^3$ if the unit of concentration $c$ is Å$^{-3}$, therefore we can rewrite $\alpha$ as $\alpha = a^3$, where $a$ can be regarded as an "effective" size. In fact, as in Fig. 2 if we can simply consider the solution as a mixture of low dielectric ion regions (say $\epsilon_m$, the same as that inside protein region, as in common MD force fields ion is cavity with a point charge and similar dielectric property as protein interior) and high dielectric water molecule region and ignore the dielectric influences from each other, supposing the $i$th ionic specie has an effective size $a_i$, the space occupancy of the low dielectric region is $\sum_{i=1}^{K} a_i^3 c_i$, and that of high dielectric region is $1 - \sum_{i=1}^{K} a_i^3 c_i$. It is worth noting here that the effective ionic size $a_i$ is not simply equal to its usual, say van der Waals (VDW), size. Considering that an ion usually has a hydration shell, in which region the relatively bounded water molecules have little freedom of reorientation and thereby much small polarizability, both the closely hydrated region and the ion occupied region have low dielectric coefficient. Therefore, a rough estimation of the effective size $a_i \sim a_i^* + a_w$, where $a_i^*$ is the ionic VDW size (diameter), and $a_w$ is water size, say 2.5 Å. We will show later in Sec. III that this consideration is reasonable, and taking $a_i = a_i^{\text{VDW}} + 2.5$ leads to good agreement with Levesque *et al.*'s[27] theory form and experimental data. Suppose the interior permittivities of ions are uniformly taken as $\epsilon_m$, then by homogenization the effective dielectric coefficient can be approximated as a linear combination of the ionic permittivity $\epsilon_m$ and water permittivity $\epsilon_w$ weighted by their volume occupancies

$$\epsilon_V^*(c_1, c_2, \ldots, c_K) = \epsilon_w - (\epsilon_w - \epsilon_m) \sum_{i=1}^{K} a_i^3 c_i. \tag{4}$$

It turns out that in monovalent ionic solution such as NaCl, $\epsilon_V^* = \epsilon_w - (\epsilon_w - \epsilon_m)(a_1^3 + a_2^3) \cdot c$, making $\alpha = (\epsilon_w - \epsilon_m)(a_1^3 + a_2^3)$ actually leads to the linear dielectric permittivity.

It is worth noting that from a rigorous physical point of view our current model only applies to electrolyte with not too high ionic concentrations. Because it is observed experimentally that in dilute solutions the dielectric decrement is linear, but at high concentrations the dielectric decrement would slow down and approach saturated, which is mainly due to ion-ion interactions.[29–32] However, in Eq. (4) the decrease rate of $\epsilon_V^*$ upon ionic concentration is constant. Therefore, for the cases of unreasonably high ionic concentrations (over saturation), the $\epsilon_V^*$ value may approach zero or even be negative. To avoid the dielectric permittivity to be unphysical values, we add a restriction to Eq. (4) to make $\epsilon_m$ as the lower bound of the calculated $\epsilon_V$. A similar linear dielectric approximation as Eq. (4) was also applied in our previous work in order to develop a molecular surface-free continuum model for studying electro diffusion processes.[33] The modified dielectric coefficient takes the form:

$$\epsilon_V(c_1, c_2, \ldots, c_K) = \begin{cases} \epsilon_m, & \text{in } \Omega_{\text{m}}, \\ \max(\epsilon_m, \epsilon_V^*), & \text{in } \Omega_{\text{s}}. \end{cases} \tag{5}$$

As can be seen in Eq. (5), $\epsilon_V$ is always less than $\epsilon_w$.

By substituting the dielectric permittivity in solution with $\epsilon_V$ and using the Boltzmann distribution $c_i = c_i^\infty e^{-\beta q_i \phi}$ in Poisson-Boltzmann equation, we obtain a VDPB equation

$$-\nabla \cdot (\epsilon_V(\phi(r))\nabla\phi(r)) = \rho^f(r) + \lambda \sum_{i=1}^{K} q_i c_i^\infty e^{-\beta q_i \phi(r)}, \text{ in } \Omega, \tag{6}$$

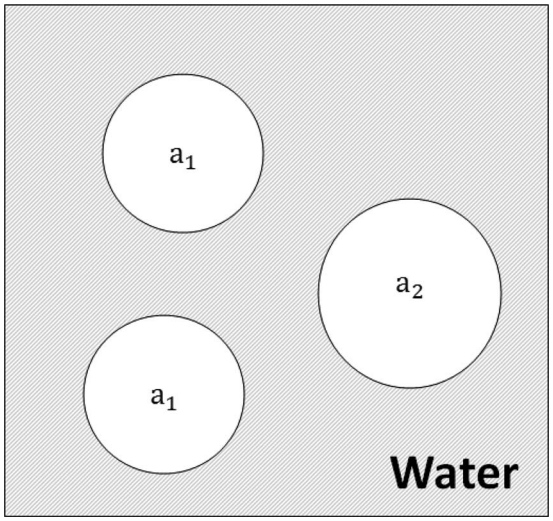


FIG. 2. Aqueous salt solution where water is mixed up with ions.

$$\epsilon_V(\phi(r)) = \begin{cases} \epsilon_m, \text{ in } \Omega_{\mathrm{m}}, \\ \max(\epsilon_m, \epsilon_w - (\epsilon_w - \epsilon_m)\sum_{i=1}^{K} a_i^3 c_i^{\infty} e^{-\beta q_i \phi(r)}), \text{ in } \Omega_{\mathrm{s}}. \end{cases}$$

Similarly, by substituting $\epsilon_V$ with $\epsilon_E$ by Levesque *et al.*[27] in PB equation, we can obtain another variable dielectric PB equation. To distinguish the two models, we will denote them by $\mathrm{VDPB}_V$ and $\mathrm{VDPB}_E$, respectively.

According to the new model, in regions far from the biomolecular surface, $c_i \approx c_i^{\infty}$, therefore $a_i^3 c_i$ is negligible, and $\epsilon \approx \epsilon_w$. Significant changes in $\epsilon$ only occurs in the vicinity of biomolecular surface where $c_i$ can be largely concentrated due to the electrostatic attraction of charged biomolecule, and $\epsilon$ can approach as low as $\epsilon_m$ as inside the solute region. Compared with traditional PB, the new models take into account the effect of dielectric decrement.

Note that for both models, dielectric permittivity $\epsilon$ depends exponentially on the electrostatic potential $\phi$. Directly solving the equation will encounter convergence difficulty. An alternative strategy is to solve PB under a given position dependent $\epsilon$, then use the solved electric potential $\phi$ to update $\epsilon$, this process is repeated until $\phi$ converges. By applying this strategy, we developed an iteration algorithm (see Table I).

As can be seen in Table I, VDPB is solved iteratively. For the $n$th iteration step, $\epsilon^n$ is dependent on $\phi^{n-1}$ only. Therefore, in each iteration step we only need to solve a regular Poisson-Boltzmann equation with a given $\epsilon(r)$.

## III. RESULTS

In this work, our results are obtained for a spherical cavity of radius 1 Å containing a central positive charge of $1e_c$, and an A-DNA duplex containing 8 base pairs and 778 atoms and a total charge of $-22e_c$.

Unless specified otherwise all calculation conditions and parameters are taken as follows. Our computation region $\Omega$ is taken as a sphere of radius 400 Å with the biomolecule at its center. The salt solution consists of 1 : 1 monovalent ions. The dielectric coefficient is set as $2\epsilon_0$ for $\epsilon_m$ and $78\epsilon_0$ for $\epsilon_w$, where $\epsilon_0$ is the vacuum dielectric permittivity. For $\mathrm{VDPB}_V$, the effective size for NaCl is set as 4.0 Å or 5.0 Å. For $\mathrm{VDPB}_E$, $\alpha$ is set as 0.278, which is the fitted value for NaCl.[28] The temperature $T$ is set as 298.15 K.

TABLE I. Iteration algorithm for VDPB.

| |
|---|
| Initialize error tolerance *tol*; |
| Initialize iterative step counter $n = 0$; |
| Initialize electric potential $\phi^0 = 0$; |
| Initialize dielectric coefficient $\epsilon^0(r) = \epsilon(\phi^0(r))$; |
| **do** |
| Determine $\phi^{n+1}$ by solving the following equation: |
| $-\nabla \cdot (\epsilon^n(r)\nabla\phi^{n+1}(r)) = \rho^f(r) + \lambda \sum_{i=1}^{K} q_i c_i^{\infty} e^{-q_i \beta \phi^{n+1}(r)}$, in $\Omega$. |
| Update the dielectric coefficient: |
| $\epsilon^{n+1}(r) = \epsilon(\phi^{n+1}(r))$. |
| n++; |
| **while** $\|\phi^{n+1} - \phi^n\| > tol$; |

Software packages TMSmesh[34] and Tetgen[35] are applied to generate the volume meshes required for finite element calculation. Our finite element solver is based on the parallel adaptive finite element package PHG.[36] The parallel code is written in C and uses MPI for message passing. The computations are carried out on the cluster LSSC-III of the State Key Laboratory of Scientific and Engineering Computing of China, which consists of compute nodes with dual Intel Xeon X5550 quad-core CPUs, interconnected via DDR InfiniBand network. Our visual program VCMM[37] is used for data analysis and visualization.

According to our numerical results listed below (see Figs. 4–8), although $\epsilon_E$ and $\epsilon_V$ are two different dielectric models, the solutions of $\mathrm{VDPB}_E$ and $\mathrm{VDPB}_V$ show some similar behaviors.

### A. Counter-ion concentration

For charged molecules in electrolyte solution, due to the existence of condensed counter-ions and hydration shells, the dielectric permittivity will be much lower than $\epsilon_w$ near the biomolecular surface (see Fig. 3). As a result, the electrostatic field near the biomolecular surface will be stronger than predicted by the traditional PB. Therefore, counter-ion concentration near the molecular surface predicted by VDPB should be higher than predicted by the traditional PB. This point of view has been supported by our numerical results. For both spherical cavity and DNA duplex, the counter-ion concentration predicted by both variable dielectric models are significantly larger than predicted by the traditional PB (see Figs. 4 and 5). Besides, for the $\mathrm{VDPB}_V$ model, the larger the size of hydration shells are taken, the faster the dielectric permittivity decreases with concentration. Therefore, the larger the size is, the higher the counter-ion concentration will be. It is worth noting that our calculations of DNA duplex agree with the studies of Pack *et al.*[21] in that changes in the dielectric coefficient for the electrolyte solution substantially increases the calculated surface concentration of counter-ions of DNA. The strong dependence of the calculated distribution of counter-ion density on the choice of dielectric coefficients representing the solvent continuum suggests that care must be taken to properly characterize the physical system when studying electrostatic properties using PB models.

### B. Charge inversion

It is worth noting that the variable dielectric coefficient may cause interesting charge compensation surrounding the biomolecule. The total compensated charges $Q$ within a given region $V$ can be calculated as

$$Q = \int_{V/\Omega_m} (q_+ c_+ + q_- c_-) dV. \tag{7}$$

As is discussed above, due to dielectric decrement, for both variable dielectric models, the counter-ion concentration will be higher and the co-ion concentration will be lower (but not significant because the magnitude of co-ion density is negligibly small) than traditional PB near the molecular surface.

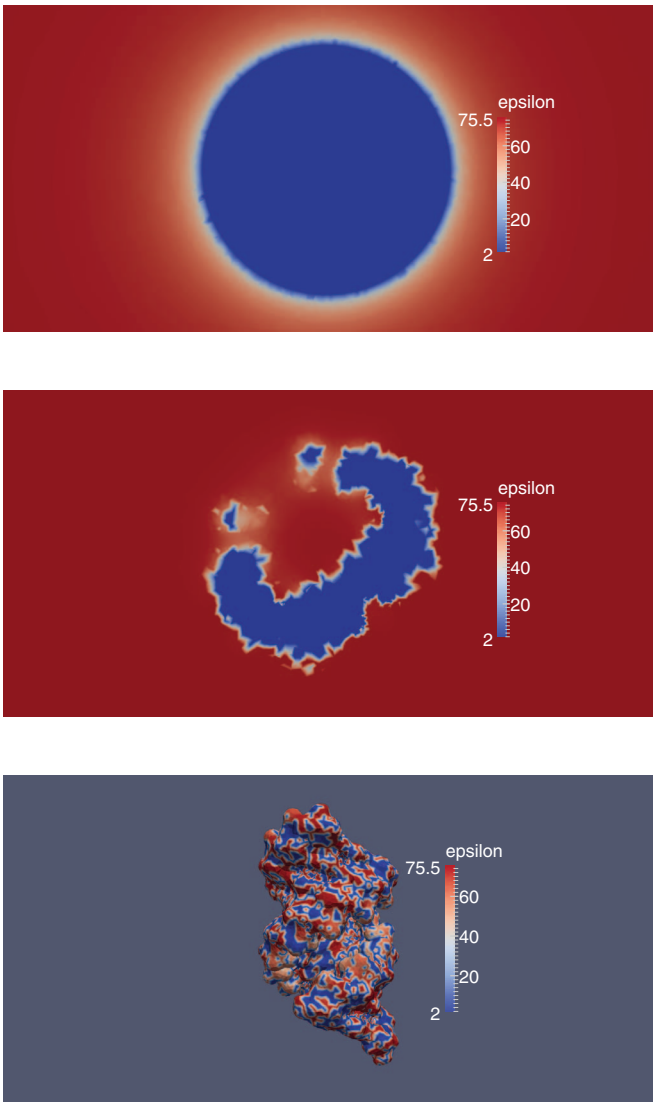


FIG. 3. The calculated dielectric permittivity distribution for $\mathrm{VDPB}_V$ around a spherical cavity is plotted in (a) and that around A-DNA is plotted in (b) and (c), all results are obtained with 1:1 salt solution at ionic strength 1M and ionic effective size 4 Å. (a) Spherical cavity, (b) A-DNA, (c) A-DNA.

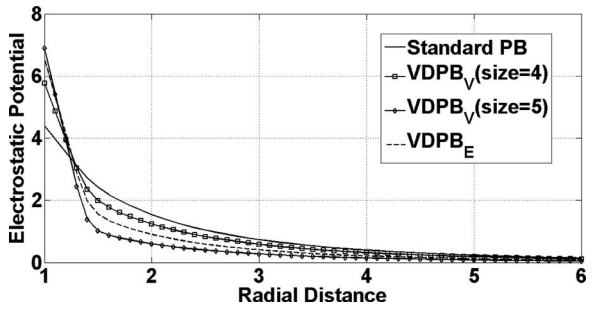


FIG. 4. The electrostatic potential, i.e., the logarithm of counter-ion concentration (in M) outside the spherical cavity in 1M NaCl solution, predicted by traditional PB, $\mathrm{VDPB}_V$ (ion size = 4, 5 Å), and $\mathrm{VDPB}_E$, are plotted against the radial distance (in Å).

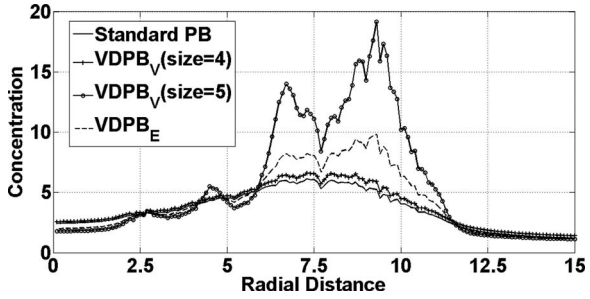


FIG. 5. The counter-ion concentration (in M) averaged over the middle of the A-DNA duplex in 1M NaCl solution, predicted by traditional PB, $\mathrm{VDPB}_V$ (ion size = 4, 5 Å), and $\mathrm{VDPB}_E$, are plotted against the radial distance (in Å).

Therefore, the total compensated charges around the molecular surface predicted by VDPBs will increase (in absolute value) compared with that obtained by the traditional PB. According to our computations, when a positive charged spherical cavity is laid in monovalent salt solution, charge inversion does not occur with the traditional PB model regardless of how much the ionic strength is. However, for the VDPB models, charge inversion can be easily observed when the ionic strength is not small (see Fig. 6).

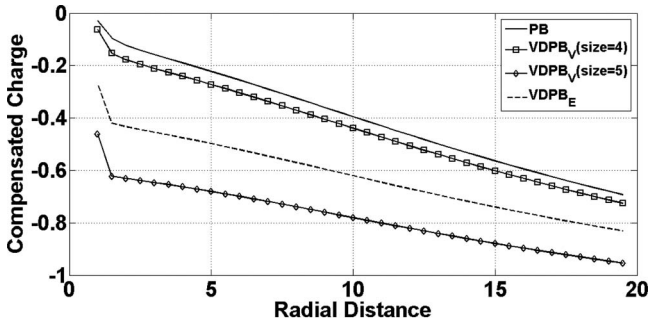


(a)

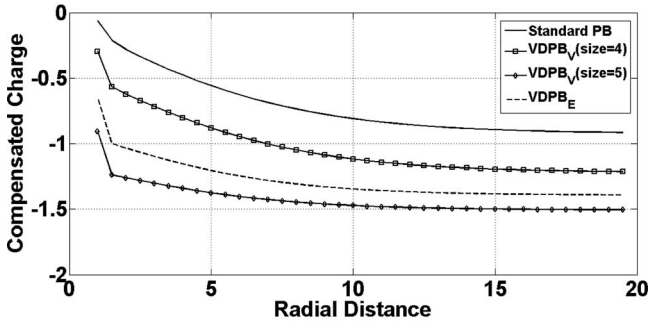


(b)

FIG. 6. The compensated charges (in $e_c$) outside the spherical cavity in monovalent salt solution of ionic strength (a) 0.1M and (b) 1M, predicted by traditional PB, $\mathrm{VDPB}_V$ (ion size = 4, 5), and $VDPB_E$, are plotted against the radial distance (in Å).

### C. Electrostatic free energy

The electrostatic free energy of a biomolecule-electrolyte solution system can be expressed as

$$G = G(\phi, c_1, c_2, \ldots, c_K) = \int_\Omega \left\{ \frac{1}{2}\left(\rho^f + \sum_{i=1}^{K} q_i c_i\right)\phi + \beta^{-1}\sum_{i=1}^{K} c_i[\ln(\Lambda^3 c_i) - 1] - \sum_{i=1}^{K}\mu_i c_i \right\} dx. \quad (8)$$

It was proved that Eq. (8) is convex and uniquely minimized by the solution of Poisson-Boltzmann.[38] Besides, the minimum value of Eq. (8) is equal to the extreme value of the expression in Eq. (9) although it is concave for all possible potentials $\phi$ and unbounded below

$$E = E(\phi) = \int_\Omega \left\{ -\frac{\epsilon}{2}|\nabla\phi|^2 + \rho^f\phi - \beta^{-1}\lambda\sum_i c_i^\infty(e^{-\beta q_i\phi} - 1) \right\} dx. \quad (9)$$

The solvation energy of a molecule (denote by $\Delta E$) is the change of energy when the molecule is taken from vacuum into a electrolyte solution

$$\Delta E = \int_\Omega \left\{ -\frac{\epsilon}{2}|\nabla\phi|^2 + \frac{1}{2}\rho^f\phi - \beta^{-1}\lambda\sum_i c_i^\infty(e^{-\beta q_i\phi} - 1) \right\} dx. \quad (10)$$

Since $E_{vacuum}$ is the same for all models considered here, solvation energy has the same property as the electrostatic free energy.

To compare the solvation energy predicted by PB and $\text{VDPB}_V$ (which we denote by VDPB for simplicity, actually all the following conclusions on solvation energy also hold true for $\text{VDPB}_E$), note that $G^{\text{VDPB}}$ is minimized by the solution of Eq. (7) and $G^{PB}$ is minimized by the solution of Eq. (3), thus we have

$$minG^{VDPB} = E^{VDPB} = E(\epsilon^{VDPB}, \phi^{VDPB}),$$
$$minG^{PB} = E^{PB} = E(\epsilon^{PB}, \phi^{PB}). \quad (11)$$

Therefore,

$$\begin{aligned} E^{VDPB} - E^{PB} &= E(\epsilon^{VDPB}, \phi^{VDPB}) - E(\epsilon^{PB}, \phi^{PB}) \\ &= E(\epsilon^{VDPB}, \phi^{VDPB}) - E(\epsilon^{PB}, \phi^{VDPB}) \\ &\quad + E(\epsilon^{PB}, \phi^{VDPB}) - E(\epsilon^{PB}, \phi^{PB}) \\ &= \int -\frac{1}{2}(\epsilon^{VDPB} - \epsilon^{PB})|\nabla\phi^{VDPB}|^2 \\ &\quad + E(\epsilon^{PB}, \phi^{VDPB}) - E(\epsilon^{PB}, \phi^{PB}). \end{aligned} \quad (12)$$

Note that $\int -\frac{1}{2}(\epsilon^{VDPB} - \epsilon^{PB})|\nabla\phi^{VDPB}|^2 \geq 0$ because $\epsilon^{VDPB} \leq \epsilon^{PB}$, and $E(\epsilon^{PB}, \phi^{VDPB}) - E(\epsilon^{PB}, \phi^{PB}) \geq 0$ because $minG^{PB} = E(\epsilon^{PB}, \phi^{PB})$. Thus $E^{VDPB} \geq E^{PB}$, this conclusion also holds true for solvation energy $\Delta E$ by subtracting a constant from both sides of Eq. (12). Therefore, we can draw a conclusion that with the same parameters, the solvation energy predicted by VDPB will always be greater than traditional PB.

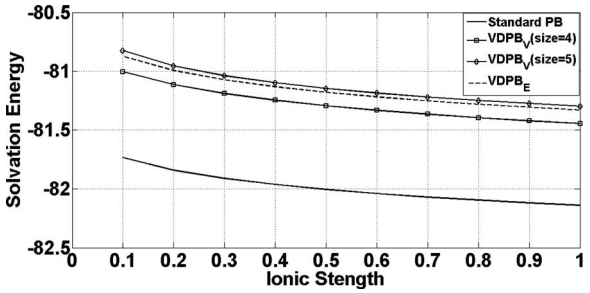


FIG. 7. The solvation energy (in kcal/mol) of spherical cavity predicted by the traditional PB, $\text{VDPB}_V$ (ion size = 4, 5 Å) and $\text{VDPB}_E$ are plotted against the ionic strength (in M).

For monovalent 1:1 salt solution, $c_+^\infty = c_-^\infty = I$. By applying variation method we have

$$\frac{\partial E^{PB}}{\partial I} = -\beta^{-1}\int_{\Omega_s}\sum_i(e^{-\beta q_i\phi} - 1) < 0, \quad (13)$$

$$\begin{aligned} \frac{\partial E^{VDPB}}{\partial I} &= -\beta^{-1}\int_{\Omega_s}\sum_i(e^{-\beta q_i\phi} - 1) \\ &\quad + \frac{\partial}{\partial I}\int -\frac{\epsilon^{VDPB}(r)}{2}|\nabla\phi|^2 \\ &= -\beta^{-1}\int_{\Omega_s}\sum_i(e^{-\beta q_i\phi} - 1) \\ &\quad + \int_{\Omega_s}\frac{\epsilon_w - \epsilon_m}{2}\sum_i a_i^3 e^{-\beta q_i\phi}|\nabla\phi|^2. \end{aligned} \quad (14)$$

Note that the first term on the right hand side of Eq. (14) takes the same form as the right hand side of Eq. (13) and is therefore negative, and the second term on the right hand side of the equation is positive. Equations (13) and (14) indicate that although the solvation energy predicted by the traditional PB model monotonically decreases as ionic strength increases, the dependence of solvation energy predicted by VDPB on ionic strength may show non-monotonic tendencies, especially for systems with strong electric field and/or under high ionic concentration condition. Such different behaviors of VDPB models are illustrated in Figs. 7 and 8.

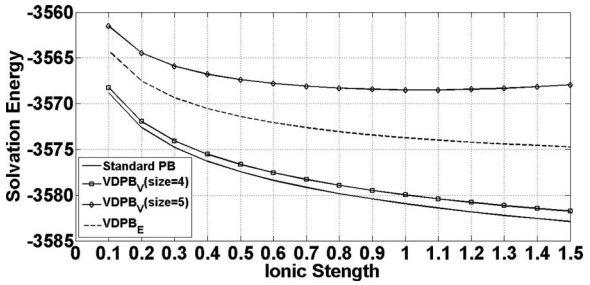


FIG. 8. The solvation energy (in kcal/mol) of A-DNA predicted by traditional PB, $\text{VDPB}_V$ (ion size = 4, 5 Å) and $\text{VDPB}_E$ are plotted against the ionic strength (in M).

As can be seen in Figs. 7 and 8, due to dielectric decrement, for both spherical cavity and DNA, the solvation energy predicted by variable dielectric models will be higher than that obtained by the traditional PB. Besides, for $VDPB_V$, the larger the size of hydration shell is taken, the larger the effective size is, and the higher the solvation energy will be.

## IV. CONCLUSION

In this work, an effort is made to find a function of dielectric permittivity in PB calculations for molecular solvation that can properly reflect the fact of dielectric decrement of electrolyte solutions. By taking into account the influence of the finite sized ions and their hydration shells on the solvent dielectric and by introducing model of Levesque *et al.*,[27] variable dielectric PB equations are obtained and applied to studies of the molecular solvation in aqueous salt solution. The $VDPB_V$ mode well explains and gives more details on the linear dielectric behavior as studied by Hasted *et al.*[24] To overcome the nonlinearity of the VDPB equations, an iterative strategy between the dielectric coefficient and the PB equation is introduced instead of using Newton method to directly solve the VDPB equations. A parallel finite element algorithm is implemented for numerical calculations. According to numerical experiments carried out for a spherical cavity and a DNA duplex, the variable dielectric models can result in considerable differences compared with the predictions of the traditional PB, especially for systems with highly charged biomolecule and/or under high salt concentration condition. The results of the variable dielectric models $VDPB_E$ and $VDPB_V$ can lead to similar deviations from those of the traditional PB. Due to dielectric decrement, counter-ion concentration near the molecular surface in VDPB calculation is found higher than that in the traditional PB. Our calculations of DNA duplex agree with the studies of Pack *et al.*[21] in that changes in the dielectric coefficient for the electrolyte solution substantially increases the calculated surface concentration of counter-ions of DNA. The variable dielectric permittivity may also influence the charge compensation behavior near biomolecular surface. For a spherical cavity solvated in a concentrated ionic solution, charge inversion occur with VDPB models, which does not occur with the traditional PB model. Besides, the solvation energy predicted by current VDPBs will always be greater than that by the traditional PB. Moreover, differing from PB, the VDPB also allows non-monotonous dependencies of solvation energy on ionic strength. According to numerical results of DNA duplex, for the $VDPB_V$ model, when the "effective" size is large enough, as the ionic strength increases, the solvation energy first decreases to a minimum then starts to increase. Such a non-monotonic phenomenon could not be observed by the traditional PB.

It is worth denoting that in VDPB model, the predicted concentrations can be either higher or lower than regular PB results, depending on the location. There are two balanced factors influencing the concentration. According to the model, a high concentration leads to low dielectric coefficient, which in turn enhances the electric field and tends to attract more counter ions. On the other hand, increased counter ion concentration leads to increased screening, which weakens the electric field and tends to lower the ionic concentration. Usually in the region very near the charged surface, the VDPB gives higher concentration prediction than the regular PB, but a bit away from the surface, the concentration can be lower than predicted by the regular PB. The phenomena is indicated by the potential profile in Fig. 4. One common disadvantage is that both the regular PB and VDPB models cannot avoid over saturated ion concentrations if the potential is high. The ion size effect is only considered in this work through its influence to the dielectric response of solvent medium, while its effects on spatial packing (volume exclusion) are not explicitly included in this model. The defects is possible to be overcome by combining VDPB with other models considering the ionic volume exclusion effects such as in the size-modified PB model[39,40] and hard sphere model,[41] which will be explored in the future and is not a focus of this work. And as aforementioned, if the concentration is really high, the new dielectric model is not suitable. In this case, it is still hard to find a good variable dielectric model so far, even for pure and homogeneously concentrated ionic solution without protein existed.

## ACKNOWLEDGMENTS

The authors thank Yan Xie, Bin Tu, Shiyang Bai, and Yu Qiao for helpful discussions and technique support on numerical algorithm, mesh generation, and visualization. This work was supported by the State Key Laboratory of Scientific/Engineering Computing, National Center for Mathematics and Interdisciplinary Sciences, the Chinese Academy of Sciences (CAS), the National Science Foundation of China (NSFC) (Grant No. 91230106), and 863 program (Grant No. 2012AA020403).

[1] M. E. Davis and J. A. McCammon, Chem. Rev. **90**, 509 (1990).
[2] F. Fogolari, A. Brigo, and H. Molinari, J. Mol. Recognit. **15**, 377 (2002).
[3] N. A. Baker, Rev. Comput. Chem. **21**, 349 (2005).
[4] A. H. Boschitsch and M. O. Fenley, J. Comput. Chem. **25**, 935 (2004).
[5] S. W. Chen and B. Honig, J. Phys. Chem. B **101**, 9113 (1997).
[6] V. K. Misra and D. E. Draper, J. Mol. Biol. **299**, 813 (2000).
[7] D. E. Draper, D. Grilley, and A. M. Soto, Annu. Rev. Biophys. Biomol. Struct. **34**, 221 (2005).
[8] C. Li, L. Li, M. Petukh, and E. Alexov, Mol. Based Math. Biol. **1**, 42 (2013).
[9] E. Allahyarov, G. Gompper, and H. Löwen, Phys. Rev. E **69**, 041904 (2004).
[10] R. W. Wilson and V. A. Bloomfield, Biochemistry **18**, 2192 (1979).
[11] A. Y. Grosberg, T. T. Nguyen, and B. I. Shklovskii, Rev. Mod. Phys. **74**, 329 (2002).
[12] G. Tresset, W. C. D. Cheong, Y. L. S. Tan, J. Boulaire, and Y. M. Lam, Biophys. J. **93**, 637 (2007).
[13] W. M. Gelbart, R. F. Bruinsma, P. A. Pincus, and V. A. Parsegian, Phys. Today **53**(9), 38 (2000).
[14] L. B. Bhuiyan, V. Vlachy, and C. W. Outhwaite, Int. Rev. Phys. Chem. **21**, 1 (2002).
[15] S. Lamperski and L. B. Bhuiyan, J. Electroanal. Chem. **540**, 79 (2003).
[16] V. N. Uversky, Intrin. Disorder. Prot. **1**, e25725 (2013).
[17] D. A. Cherepanov, B. A. Feniouk, W. Junge, and A. Y. Mulkidjanian, Biophys. J. **85**, 1307 (2003).
[18] O. Teschke, G. Ceotto, and E. De Souza, Phys. Rev. E **64**, 011605 (2001).
[19] L. Vrbka, M. Lund, I. Kalcher, J. Dzubiella, R. R. Netz, and W. Kunz, J. Chem. Phys. **131**, 154109 (2009).
[20] W. C. Guest, N. R. Cashman, and S. S. Plotkin, Phys. Chem. Chem. Phys. **13**, 6286 (2011).
[21] G. R. Pack, G. Garrett, L. Wong, and G. Lamm, Biophys. J. **65**, 1363 (1993).

[22]L. Li, C. Li, Z. Zhang, and E. Alexov, J. Chem. Theory Comput. **9**, 2126 (2013).
[23]M. Petukh, M. Zhenirovskyy, C. Li, L. Li, L. Wang, and E. Alexov, Biophys. J. **102**, 2885 (2012).
[24]J. Hasted, D. Ritson, and C. Collie, J. Chem. Phys. **16**, 1 (1948).
[25]E. Glueckauf, Trans. Faraday Soc. **60**, 1637 (1964).
[26]J. Liszi, A. Felinger, and E. H. Kristóf, Electrochim. Acta **33**, 1191 (1988).
[27]D. Levesque, J. Weis, and G. Patey, J. Chem. Phys. **72**, 1887 (1980).
[28]B. Hess, C. Holm, and N. van der Vegt, Phys. Rev. Lett. **96**, 147801 (2006).
[29]Y.-Z. Wei and S. Sridhar, J. Chem. Phys. **92**, 923 (1990).
[30]Y.-Z. Wei, P. Chiang, and S. Sridhar, J. Chem. Phys. **96**, 4569 (1992).
[31]R. Buchner, G. T. Hefter, and P. M. May, J. Phys. Chem. A **103**, 1 (1999).
[32]H. Weingärtner, A. Knocks, W. Schrader, and U. Kaatze, J. Phys. Chem. A **105**, 8646 (2001).
[33]B. Lu and J. A. McCammon, Chem. Phys. Lett. **451**, 282 (2008).
[34]M. Chen and B. Lu, J. Chem. Theory Comput. **7**, 203 (2011).
[35]H. Si, *TetGen: A Quality Tetrahedral Mesh Generator and 3D Delaunay Triangulator* (Weierstrass Institute for Applied Analysis and Stochastic, Berlin, Germany, 2006).
[36]L.-B. Zhang, Numer. Math. Theory Methods Appl. **2**, 65 (2009).
[37]S. Bai and B. Lu, J. Mol. Graph. Modell. **50**, 44 (2014).
[38]J. Che, J. Dzubiella, B. Li, and J. A. McCammon, J. Phys. Chem. B **112**, 3058 (2008).
[39]I. Borukhov, D. Andelman, and H. Orland, Phys. Rev. Lett. **79**, 435 (1997).
[40]Y. Qiao, B. Tu, and B. Lu, J. Chem. Phys. **140**, 174102 (2014).
[41]Y. Rosenfeld, J. Chem. Phys. **93**, 4305 (1990).